Available online at www.sciencedirect.com
SCIENCE DIRECT®
Journal of Theoretical Biology 223 (2003) 367–375
Journal of Theoretical Biology
www.elsevier.com/locate/jtbi

The relationship between neuronal calcium concentration and firing rate during stochastic synaptic inputs

Jianfeng Feng[a,b,*], Guibin Li[b]

[a] COGS, Sussex University, Brighton BN1 9QH, UK
[b] Computational Neuroscience Laboratory, The Babraham Institute, Cambridge CB2 4AT, UK

Received 5 September 2001; received in revised form 6 January 2003; accepted 26 February 2003

Abstract

We propose a novel, nonlinear theory about reading neuronal information using intracellular calcium concentrations, which includes the linear theory already developed in the literature as a special case. The theory is numerically confirmed using the Pinsky–Rinzel and integrate-and-fire models with constant rate Poisson inputs. Applying the theory to models with non-constant inputs, we find that there is a time lag equal to the calcium buffering time constant between the instantaneous firing rate and the firing rate estimated using calcium concentrations.

Keywords: Calcium concentration; Instantaneous firing rate; The Pinsky–Rinzel model; The integrate and fire model

1. Introduction

Ca^{2+} is a ubiquitous intracellular messenger, controlling many activities in neuronal systems, as has been amply demonstrated both in modelling and experiment work [see, for example, Jafri and Yang (2003) for a recent review]. For example, in LeMasson et al. (1993), under the assumption that maximal conductances of ionic currents depend on the intracellular calcium concentration, the model considered there shows stable behaviour. Berridge (1998) proposed that the neuronal endoplasmic reticulum, served as a store of intracellular calcium, could manipulate a wide range of processes such as excitability, neurotransmitter release, plasticity, etc. In all the theory above, the essential assumption is that the electric activity of neurons can be read out by an observation of the intracellular calcium activity, and vice versa.

In recent years, a linear theory which asserts that the efferent firing rate of neuron is a linear function of intracellular calcium concentration has been developed in models (Wang, 1998), in theory (Ermentrout, 1998) and in experiments (Helmchen et al., 1996). In particular, in Ermentrout (1998), it is shown that the linear relationship between firing rate and input occurs because of the negative feedback in neuronal models. The linear relationship between efferent firing rate and calcium concentration is the simplest way to read out the information which is routinely thought as being encoded in interspike intervals. In fact, from the time of Bernard (1878), it has been assumed that physiological systems possess feedback and control mechanisms that serve to restore an equilibrium state when the system is perturbed away from some set point and therefore a linear theory is applicable.

However, in general it would be natural to expect that the relationship between calcium concentrations and neuronal activity is not linear, or indeed any system is inherently out-of-equilibrium, as been demonstrated in recent years developments in physics. In the present paper we develop such a nonlinear theory, which includes the linear theory as a special case. The nonlinear theory developed here gives us the exact relationship between the efferent firing rate and intracellular calcium concentrations. To confirm our theory, we modify the integrate-and-fire (IF) model by adding a calcium current, and consider the Pinsky–Rinzel (PR) model with stochastic synaptic inputs.

*Corresponding author. Biomathematics Laboratory, the Babraham Institute, Cambridge CB2 4AT, UK. Tel.: +44-1223-496-254; fax: +44-1223-496-020.
E-mail address: jf218@cam.ac.uk (J. Feng).
URL: http://www.cus.cam.ac.uk/~jf218.

0022-5193/03/$ - see front matter © 2003 Elsevier Ltd. All rights reserved.
doi:10.1016/S0022-5193(03)00115-2

Within a quite wide range of parameters, the theory fits well with numerical simulations. Using the theory, we then determine when neuronal information can be read out using calcium concentrations. To this end, the PR model with non-constant synaptic inputs is considered. Our results show that there is always a time lag between the true firing rate and the firing rate estimated using the intracellular calcium concentration, as demonstrated in Smith et al. (2001) with deterministic inputs.

2. Models

2.1. Calcium dynamics

Let $[Ca^{2+}] = [Ca^{2+}](t)$ be the intracellular calcium concentration at time t. For the simplicity of notation we model calcium buffering as a linear decay with a time constant τ_{Ca} (buffering time constant)

$$\frac{d[Ca^{2+}]}{dt} = -\frac{[Ca^{2+}]}{\tau_{Ca}} - \alpha I_{Ca},$$

$$I_{Ca} = g_{Ca}\frac{V - V_{Ca}}{1 + \exp[-(V+\xi)/\eta]}, \tag{2.1}$$

where V is membrane potential of the IF neuron, $\alpha > 0, \xi > 0, \eta > 0$ are all positive constants, g_{Ca} is the maximum conductance, and V_{Ca} is the reversal potential of calcium channels in the IF model.

For the Pinsky–Rinzel (PR) model, as in Pinsky and Rinzel (1994), we use the following calcium dynamics for the dendritic compartment:

$$\frac{d[Ca^{2+}]}{dt} = -\frac{[Ca^{2+}]}{\tau_{Ca}} - \alpha I_{Ca},$$

$$I_{Ca} = g_{Ca}s^2(V - E_{Ca}),$$

$$s' = (s_\infty - s)/\tau, \tag{2.2}$$

where V is the dendritic compartment membrane potential $s_\infty = \alpha/(\alpha+\beta)$, $\tau = 1/(\alpha+\beta)$ with

$$\alpha = \frac{1.6}{1 + \exp(-0.072(V - 65))},$$

$$\beta = \frac{0.02(V - 51.1)}{\exp((V - 51.1)/5) - 1}$$

and E_{Ca} is the reversal potential of calcium channels in the PR model.

2.2. The IF model

Suppose that a neuron receives N_E excitatory inputs each following a Poisson process of density λ_E, and N_I inhibitory inputs which are Poisson process of density λ_I. Let a, b be EPSP and IPSP sizes. We first consider the following integrate-and-fire model without reversal potentials.

$$dV = -\frac{V - V_{rest}}{\gamma}dt - I_{Ca}\,dt + dI_{syn}, \tag{2.3}$$

where I_{Ca} is defined as in the previous section, V_{rest} is the resting potential, and $I_{syn} = \mu t + \sigma B_t$ with B_t as the standard Brownian motion and

$$\mu = aN_E\lambda_E - bN_I\lambda_I,$$

$$\sigma^2 = a^2N_E\lambda_E + b^2N_I\lambda_I. \tag{2.4}$$

When V crosses the threshold V_{th} from below, a spike is generated and V is reset to V_{rest}. We use $g_{Ca} = 0.1, 0.05$ in the following numerical simulations. Other parameters are $a = b = 0.5$ mV, $N_E = N_I = 100$, $\lambda_E = 100$ Hz, $\lambda_I = 0, 10, 20, \ldots, 100$ Hz, $V_{rest} = -50$ mV, $V_{th} = -30$ mV, $\xi = 20$, $\eta = 9$, $V_{Ca} = 120$. Hence all simulations are carried out when the neuron receives inputs ranging from purely excitatory input ($\lambda_I = 0$) to exactly balanced inhibitory inputs and excitatory inputs ($\lambda_I = 100$ Hz). For discussions on the choice of these parameters, we refer the reader to publications (Brown et al., 1999; Feng, 1997) and references therein.

For a further comparison we also consider the following integrate-and-fire model with reversal potentials

$$dV = -\frac{V - V_{rest}}{\gamma}dt - I_{Ca}\,dt + d\bar{I}_{syn}, \tag{2.5}$$

where I_{Ca} is defined as in the previous section, V_{rest} is the resting potential, and $\bar{I}_{syn} = \mu t + \sigma B_t$ with

$$\mu = aN_E\lambda_E(V - V_E) - bN_I\lambda_I(V - V_I),$$

$$\sigma^2 = a^2N_E\lambda_E(V - V_E)^2 + b^2N_I\lambda_I(V - V_I)^2.$$

When V crosses the threshold V_{th} from below, a spike is generated and V is reset to V_{rest}. Parameters are $g_{Ca} = 0.1, 0.05$, $a = 0.01$ mV, $b = 0.1$ mV, $N_E = N_I = 100, \lambda_E = 100$ Hz, $\lambda_I = 0, 10, 20, \ldots, 100$ Hz, $V_{rest} = -50$ mV, $V_{th} = -30$ mV, $V_E = 50$ mV, $V_I = -60$ mV.

For constant rate inputs the interspike interval (ISI) T of the IF model is defined by

$$T = \inf\{V \geqslant V_{th}, V(0) = V_{rest}\}. \tag{2.6}$$

2.3. PR model

All parameters of the PR model are identical to those used in Pinsky and Rinzel (1994) with $E_{Ca} = 140$ mV except that α and τ_{Ca} are the same as in Wang (1998); Helmchen et al. (1996), which is measured in recent experiments (see below).

$$C_m\,dV_s = -I_L(V_s)\,dt - I_{Na}(V_s, h)\,dt - I_K(V_s, n)\,dt + \frac{g_c}{p}(V_d - V_s)\,dt,$$

$$C_m\,dV_d = -I_L(V_d)\,dt - I_{Ca}(V_d,s)\,dt - I_{AHP}(V_d,q)\,dt - I_{K(Ca)}(V_d,Ca,c)\,dt + \frac{g_c}{1-p}(V_s-V_d)\,dt + \frac{I_s}{1-p} + dI_{syn}, \quad (2.7)$$

where $I_s = 0.75\ \mu A/cm^2$. Note that the PR model is a two-compartment model, with a somatic compartment and a dendritic compartment, which is a simplification of a more complex pyramidal cell model (Pinsky and Rinzel, 1994). Depending on p, the ratio between somatic area with respect to the whole cell membrane area, the model can exhibit bursting and single spike activity (Feng and Li, 2001).

Synaptic input is I_{syn} as defined above. Numerical simulations were carried out on Dec Alpha workstations using the NAG numerical library. In particular the PR model is solved using a Runge–Kutta method with variable stepsize.

3. ISI and calcium concentration

3.1. Preliminary results

Suppose that the neuron fires at times $0 = T_0 < T_1 < T_2 < \cdots < T_N$. Solving Eq. (2.1) [similar for Eq. (2.2)] we obtain

$$[Ca^{2+}] = \alpha g_{Ca}\sum_{i=0}^{N-1}\exp(-(t-T_i)/\tau_{Ca}) \times \int_0^{T_{i+1}-T_i}\exp(s/\tau_{Ca})\frac{(V_{Ca}-V)}{1+\exp[-(V+\xi)/\eta]}\,ds + \alpha g_{Ca}\int_{T_N}^{t}\exp(-(t-s)/\tau_{Ca}) \times \frac{(V_{Ca}-V)}{1+\exp[-(V+\xi)/\eta]}\,ds. \quad (3.1)$$

According to the Law of Large Numbers we have that $T_i/i \to \langle T\rangle$ when $i\to\infty$, where T is the interspike interval. The right-hand side of the equation above thus becomes

$$\alpha g_{Ca}\sum_{i=0}^{N-1}\left[\exp(-(t-i\langle T\rangle)/\tau_{Ca})\int_0^{T_{i+1}-T_i}\exp(s/\tau_{Ca}) \times \frac{(V_{Ca}-V)}{1+\exp[-(V+\xi)/\eta]}\,ds\right]. \quad (3.2)$$

Taking expectation on both sides of the equation above and using $\langle Ca^{2+}\rangle$ for its mean, we obtain

$$\langle Ca^{2+}\rangle = C\frac{(1-\exp(-N\langle T\rangle_e/\tau_{Ca}))}{\exp(\langle T\rangle_e/\tau_{Ca}-1)}, \quad (3.3)$$

where

$$C = C(\langle Ca^{2+}\rangle) = -\alpha\left\langle\int_0^T \exp(s/\tau_{Ca})I_{Ca}\,ds\right\rangle \quad (3.4)$$

the average weighted calcium current with the weight $\exp(t/\tau_{Ca})$, and $\langle T\rangle_e$ represents the estimated average interspike intervals satisfying Eq. (3.3). The constant C will play an important role in the following development.

If we further assume that t is large enough, in Eq. (3.3) the term

$$\exp(-t/\tau_{Ca}) \sim 0.$$

Hence Eq. (3.3) is further reduced to

$$\langle Ca^{2+}\rangle = \frac{C}{\exp(\langle T\rangle_e/\tau_{Ca})-1}$$

which implies the following nonlinear relation between calcium concentration and average interspike intervals

$$\langle T\rangle_e = \tau_{Ca}\log\left(1+\frac{C}{\langle Ca^{2+}\rangle}\right). \quad (3.5)$$

Under the condition that $\frac{C}{[Ca^{2+}]}$ is small, we obtain

$$\langle T\rangle_L = \frac{C\tau_{Ca}}{\langle Ca^{2+}\rangle}, \quad F_L = \frac{[Ca^{2+}]}{\tau_{Ca}C} \quad (3.6)$$

a linear relationship between calcium concentration and firing frequency F_L provided that C is independent of $\langle Ca^{2+}\rangle$ [see Fig. 1, on page 1551 of Wang (1998)].

Note that the Law of Large Numbers is true not only for the i.i.d case, but also for the stationary case. Hence all conclusions above are also valid for interspike intervals with correlations, which is the case for some biophysical models and experimental data.

Now we have three quantities $\langle T\rangle_L, \langle T\rangle_e$ and $\langle T\rangle$. What is the relationship between them? It is easily seen that

$$\langle T\rangle_L \geqslant \langle T\rangle_e$$

since $x \geqslant \log(1+x)$ for $x \geqslant 0$. Under the condition that interspike intervals are independent, Eq. (3.1) is

$$\langle Ca^{2+}\rangle = C\left\langle\exp(-t/\tau_{Ca})\sum_{i=0}^{N-1}\exp(T_i/\tau_{Ca})\right\rangle \geqslant C\exp(-t/\tau_{Ca})\sum_{i=0}^{N-1}\exp(i\langle T\rangle/\tau_{Ca}) \quad (3.7)$$

since $\exp(x)$ is a convex function. We thus obtain the following conclusion:

$$\langle T\rangle_L \geqslant \langle T\rangle_e \geqslant \langle T\rangle. \quad (3.8)$$

The linear estimate $\langle T\rangle_L$ is an upper bound of the true value and nonlinear estimate $\langle T\rangle_e$. The nonlinear estimate is again an upper bound of the true value, but it gives a better estimate than the linear one.

Numerical results of $\langle T\rangle_L, \langle T\rangle_e$, and $\langle T\rangle$ of the IF model without reversal potentials are shown in Fig. 1, upper panel. It is readily seen that both $\langle T\rangle_L$ and $\langle T\rangle_e$ give a reasonable estimate of $\langle T\rangle$ when the inputs are away from exact balance ($\lambda_I \leqslant 90$ Hz). However a discrepancy is observed when exactly

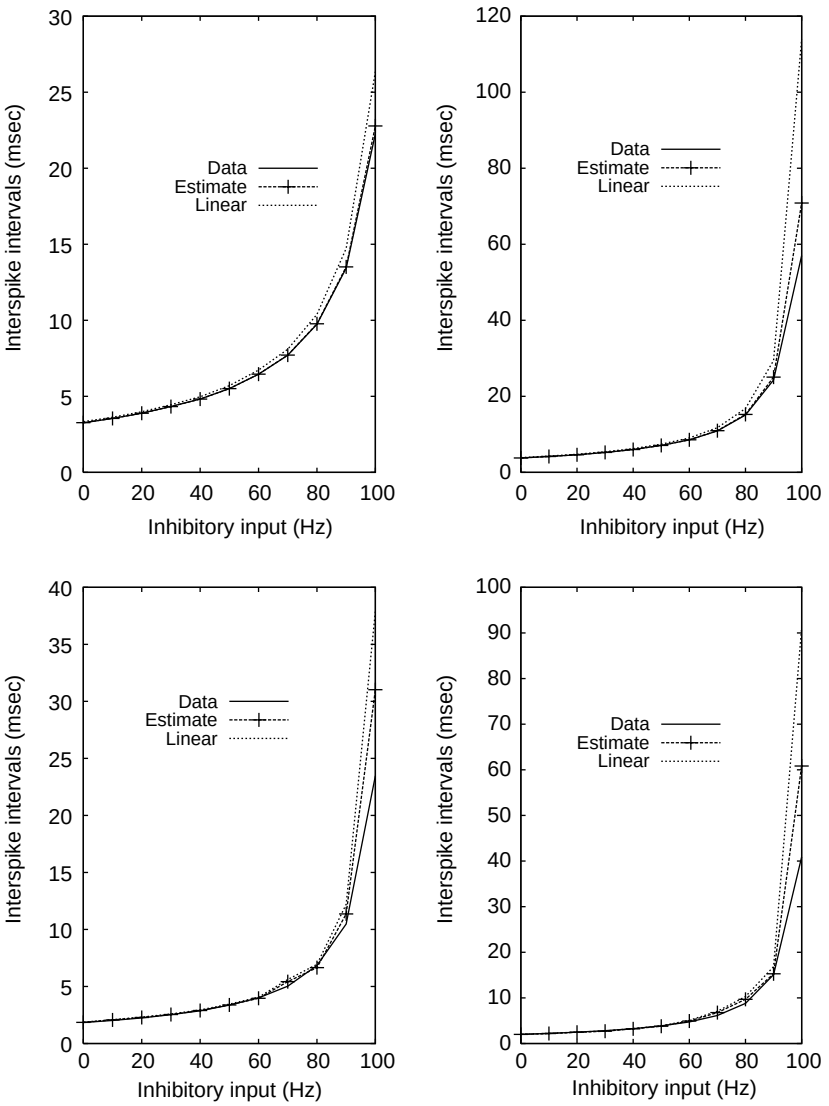

Fig. 1. $\langle T\rangle_L$ (Linear), $\langle T\rangle_e$ (estimate), and $\langle T\rangle$ (Data) vs. λ_I. Upper panel, the IF model without reversal potentials with $g_{Ca} = 0.1$ (left), $g_{Ca} = 0.05$ (right). See content for other parameters. Bottom panel, the IF model with reversal potentials with $g_{Ca} = 0.1$ (left), $g_{Ca} = 0.05$ (right).

balanced inputs are presented ($\lambda_I = 100$ Hz). The relationship $\langle T\rangle_L \geqslant \langle T\rangle_e \geqslant \langle T\rangle$ is true. Fig. 1, bottom panel shows numerical results of $\langle T\rangle_L$, $\langle T\rangle_e$, and $\langle T\rangle$ of the IF model with reversal potentials. As in the case of the IF model without reversal potentials, $\langle T\rangle_L$, $\langle T\rangle_e$, and $\langle T\rangle$ agree well with each other when the inputs are away from exact balance. Furthermore we have the relationship $\langle T\rangle_L \geqslant \langle T\rangle_e \geqslant \langle T\rangle$.

In Fig. 2, upper panel the numerical results for $\langle T\rangle_L$, $\langle T\rangle_e$, and $\langle T\rangle$ of the PR model without reversal potentials are given. As in the case of the IF model, $\langle T\rangle_L$, $\langle T\rangle_e$, and $\langle T\rangle$ agree well with each other when inputs are away from exact balance. When $p = 0.5$, i.e. somatic area is equal to dendritic area, mean firing time of somatic and dendritic compartments are almost identical. Increasing the somatic area will ensure the two compartments fire at identical times. What then is the effect of reducing p? Fig. 2, bottom panel shows the numerical results. It is interesting to note that the discrepancy in firing rate between somatic and dendritic compartments increases, compared to $p \geqslant 0.5$. However, dendritic calcium can predict somatic activity and the prediction is still very good.

4. Linear response theory

As we have pointed out, when C defined in Eq. (3.3) is a constant independent of $\langle Ca^{2+}\rangle$, a linear relationship between the output frequency and the calcium concentration is obtained, as reported in Wang (1998), Ermentrout (1998). Now we check that whether the linear relationship is true, and if it is not, we investigate how to generalize it.

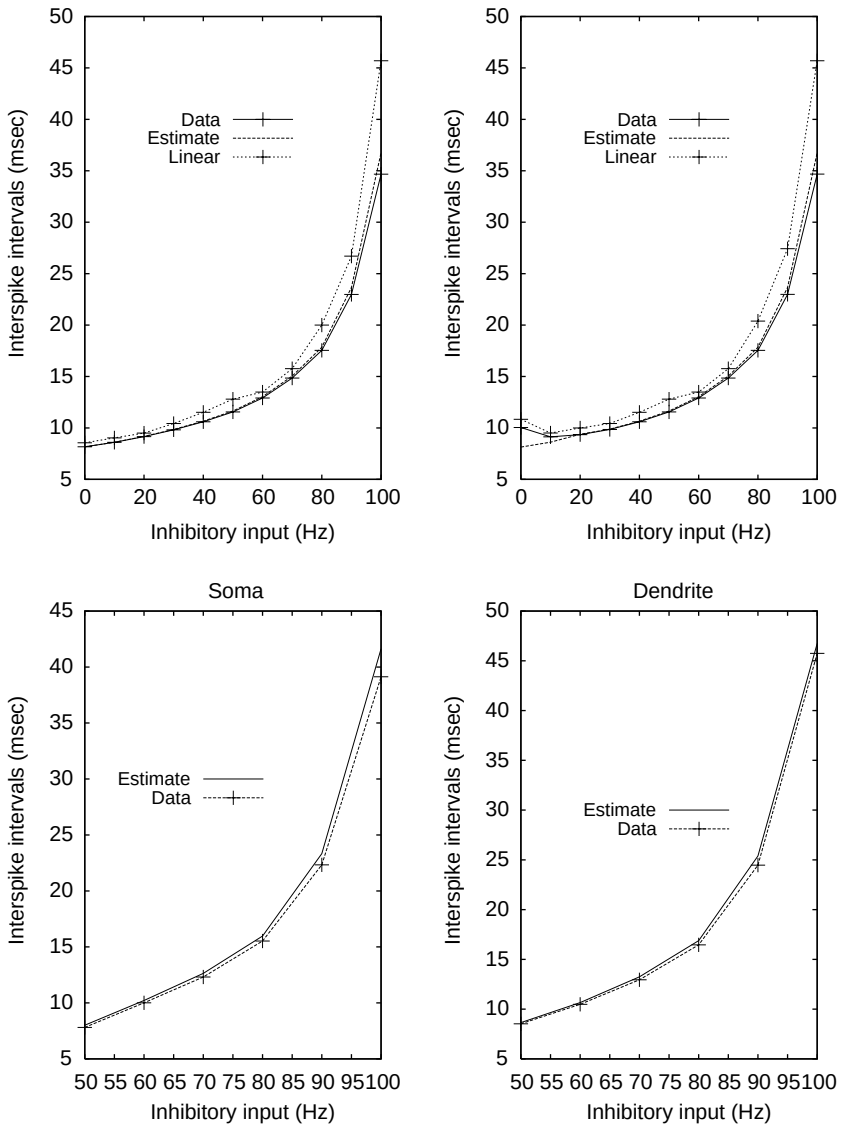

Fig. 2. $\langle T\rangle_L$ (Linear), $\langle T\rangle_e$ (estimate), and $\langle T\rangle$ (Data) of the PR model vs. λ_I with $g_{Ca} = 0.5$. Upper panel, $p = 0.5$, Somatic compartment (Left) and dendritic compartment (Right). Bottom panel, $p = 0.3$. Although there is a discrepancy between the firing rate of the somatic compartment and dendritic compartment, our theoretical results give rise to a reasonable estimate.

The simplest generalization involves the application of the linear response theory to estimate the constant C. By this we mean that C is a linear function of the calcium concentration, i.e.

$$C = C_1 + C_2\langle \mathrm{Ca}^{2+}\rangle. \tag{4.1}$$

Eq. (3.5) now becomes

$$\langle T\rangle_e = \tau_{\mathrm{Ca}} \log\left(1 + C_2 + \frac{C_1}{\langle \mathrm{Ca}^{2+}\rangle}\right),$$

$$F_e = 1\Big/\left[\tau_{\mathrm{Ca}}\log\left(1 + C_2 + \frac{C_1}{\langle \mathrm{Ca}^{2+}\rangle}\right)\right]. \tag{4.2}$$

To check our theory above, we fit simulated data with Eq. (4.2) for all figures presented in the previous section (Figs. 1 and 2). It is easily seen that $\bar{C}_2$ is not negligible in all figures (Figs. 3 and 4) and therefore the linear relationship between the firing rate and calcium concentrations is not true.

Finally we emphasize that the linear response theory is applied to the constant C, rather than the relationship between the firing frequency and calcium concentration, which is not linear provided that $\bar{C}_1 \neq 0$ and $\bar{C}_2 \neq 0$. We could of course expand C into further order of Ca^{2+} and improve the estimation.

5. Nonconstant inputs

In the previous sections, we have presented a nonlinear theory to predict the firing rate from calcium concentrations. However, we confine ourselves to the

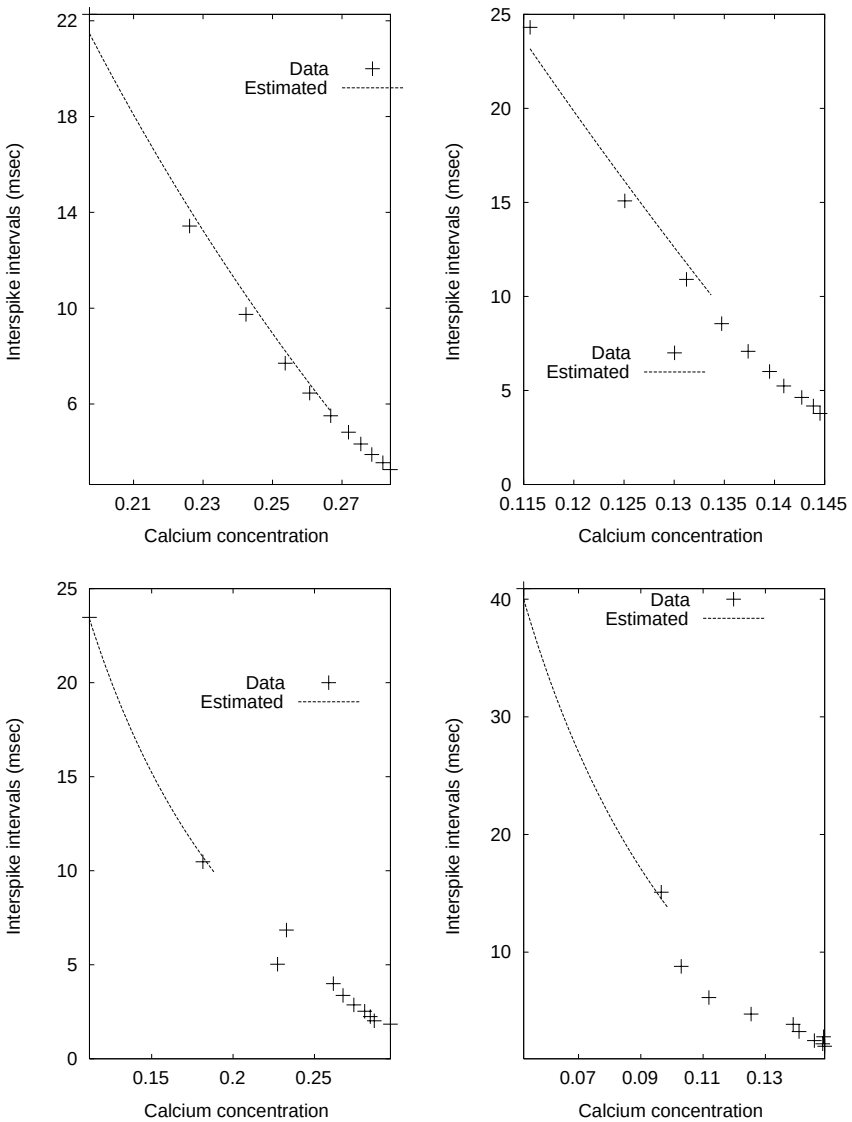

Fig. 3. Mean interspike interval vs. calcium concentration (μM). Upper panel, the IF model without reversal potentials (see Fig. 1, upper panel). Left, Estimated $= \tau_{Ca} \log(0.4088 + 0.17739/\langle Ca^{2+} \rangle)$; Right, Estimated $= \tau_{Ca} \log(0.6664 + 0.05147/\langle Ca^{2+} \rangle)$. Bottom panel, the IF model with reversal potentials (see Fig. 1, bottom panel). Left, Estimated $= \tau_{Ca} \log(0.82888 + 0.05710/\langle Ca^{2+} \rangle)$; Right, Estimated $= \tau_{Ca} \log(0.6664 + 0.05147/\langle Ca^{2+} \rangle)$.

case of constant rate input, which is of purely theoretical interest. In this section, we turn to a more realistic case: the PR model subjected to non-constant rate inputs. More exactly we assume that

$$\lambda_E(t) = 100 \text{ Hz},$$

$$\lambda_I(t) = 0.05(1.0 + \cos(2\pi t/1000.0)) \times 100 \text{ Hz}$$

with $a = 1$ mV, $b = 1$ mV, $N_E = N_I = 40$ for $p = 0.5$. Therefore according to Eq. (2.4) the mean input signal (see Fig. 5) is

$$\text{Input signal} = 4 - 2(1. + \cos(2\pi t/1000.0)). \tag{5.1}$$

Note that the parameter set we use here is very different from the one we used in the previous section for estimating the relationship between firing rate and calcium concentration, Fig. 4. From Fig. 5, upper panel we see that there is a delay for the firing rate estimated in terms of the calcium concentrations. After shifting it to the left with a time of 80 ms, it agrees reasonably well with the firing rate calculated directly from the spike train. A time lag, which is proportional to the calcium time constant τ_{Ca}, occurs. We also simulate the PR model with $\tau_{Ca} = 40$ ms (Fig. 5, bottom panel) and $\tau_{Ca} = 1$ ms (not shown). For the case $\tau_{Ca} = 40$ ms, a time lag of 40 ms is observable between data and estimated data, but not for $\tau_{Ca} = 1$ ms. Therefore, we conclude that to read out neuronal information using calcium concentrations depends on the buffering time constant, at least for the models we consider here.

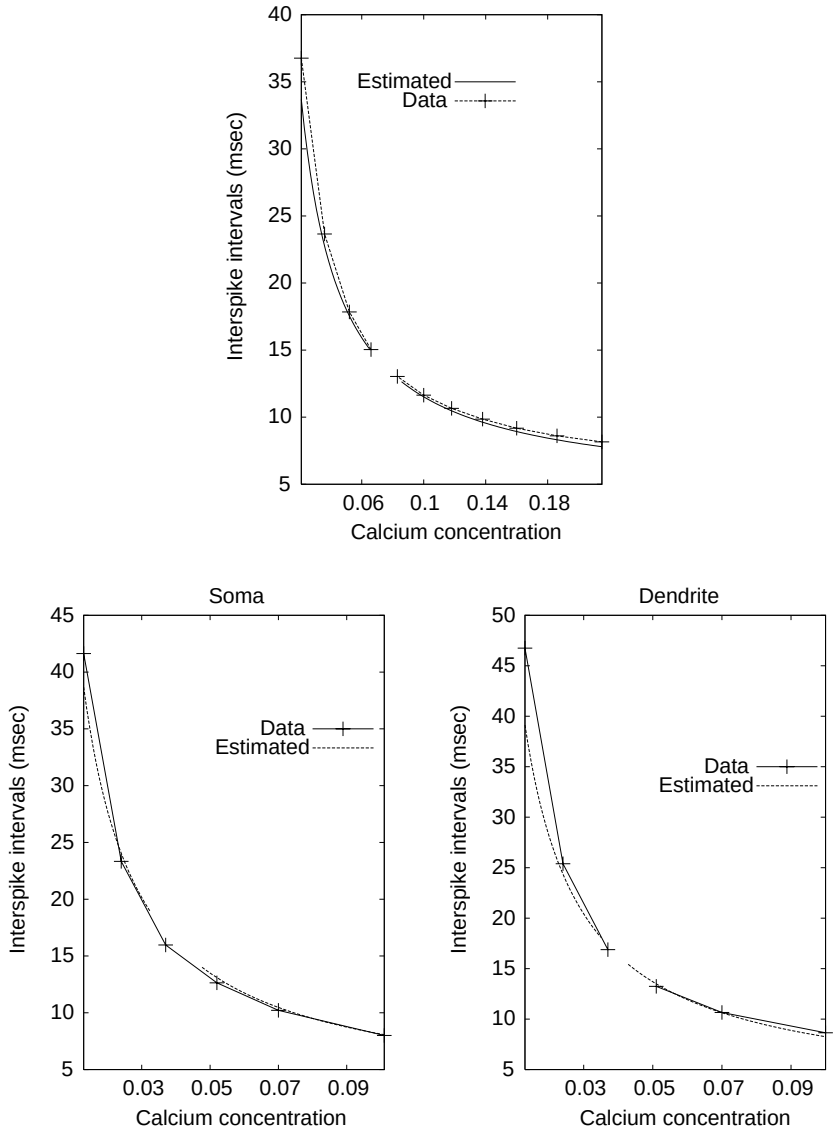

Fig. 4. Mean interspike interval vs. calcium concentration for the PR model. Upper panel, $p = 0.5, g_{Ca} = 0.5$. Only results of the somatic compartment are shown here (see Fig. 2, upper panel) Estimated $= \tau_{Ca} \log(1.05682 + 0.0098/\langle Ca^{2+} \rangle)$. Bottom panel, $p = 0.3$ (Comparing Fig. 2, bottom panel). Dendrite, Estimated $= \tau_{Ca} \log(1.03070 + 0.007803/\langle Ca^{2+} \rangle)$; soma, Estimated $= \tau_{Ca} \log(1.030024 + 0.007691/\langle Ca^{2+} \rangle)$.

6. Discussion

We have investigated the behaviour of the calcium concentration in two different simple spiking models: an integrate-and-fire model with added calcium current and the Pinsky–Rinzel model, when driven by Poisson synaptic inputs, both homogeneous and inhomogeneous. The estimation of the firing rate from the calcium concentration is developed, and demonstrated across a range of ratios of the inhibitory:excitatory input. Using inhomogeneous (sinusoidal) rates of input, it is shown by numerical simulations that the estimator produces a delayed version of the actual firing rate, with a delay proportional to the time constant for clearing calcium.

Our results indicate that an on-line reading of the firing rate is impossible. In fact, any reading out of neuronal information has to involve a physical process, with an associated delay. It is like showing that it is impossible to read out synaptic current on-line because there is a lag involved in charging up the membrane capacitance. What is interesting about the delay is not that it exists, but how big it is, how it depends on the parameters, and perhaps also how one might construct a better predictive estimator of the firing rate to deal with this.

There are many other interesting issues which need to be further explored. For example, whether we can predict higher order statistics of interspike intervals using calcium concentration. Furthermore, we here

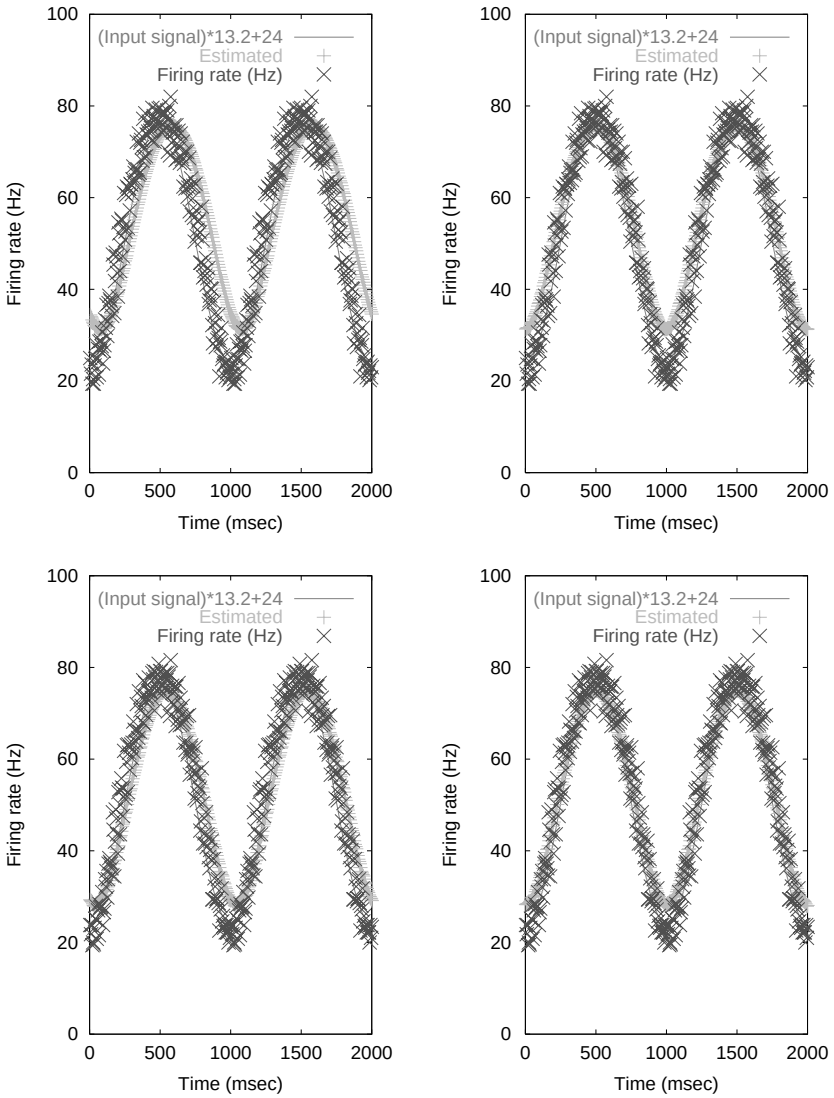

Fig. 5. Instantaneous firing rate vs. time (ms). Firing rates are obtained from spike trains with a bin of 5 ms. Data of 1000 s are generated for calculating firing rate and calcium concentrations. Input signal is defined by Eq. (5.1). $p = 0.5, g_{Ca} = 0.5$. Upper panel, $\tau_{Ca} = 80$ ms. Right: with a shift of 80 ms for the firing rate estimated in terms of $\tau_{Ca} \log(1.05682 + 0.0098/\langle Ca^{2+} \rangle)$, see Fig. 4. Bottom panel, $\tau_{Ca} = 40$ ms. Right: with a shift of 40 ms for the firing rate estimated in terms of $1000./[\tau_{Ca} \log(1.0683 + 0.013542/\langle Ca^{2+} \rangle)]$.

modelled calcium buffer simply as a linear decay, which is approximately true for certain situations. How to generalize our results to more realistic model including nonlinear buffers (De Schutter and Smolen, 1998) would be interesting.

Acknowledgements

We are grateful to two referees for their valuable comments, and for one of them to bring (Smith et al., 2001) to our attention. The work was financially supported by grants from EPSRC (GR/R54569/01) and EPSRC (GR/16813), a grant of the Royal Society and an exchange grant between UK and China of the Royal Society.

References

Bernard, C., 1878. Les Phenomenes de la vie. Paris.

Berridge, M.J., 1998. Neuronal calcium signaling. Neuron 21, 13–26.

Brown, D., Feng, J.F., Feerick, S., 1999. Variability of firing of Hodgkin–Huxley and FitzHugh–Nagumo neurones with stochastic synaptic input. Phys. Rev. Lett. 82, 4731–4734.

Ermentrout, B., 1998. Linearization of F-I curves by adaptation. Neural Comput. 10, 1721–1729.

Feng, J.F., 1997. Behaviours of spike output jitter in the integrate-and-fire model. Phys. Rev. Lett. 79, 4505–4508.

Feng, J.F., Li, G.B., 2001. Impact of geometrical structures on the output of neuronal models—a theoretical and numerical analysis. Neural Comput. 14, 621–640.

Helmchen, F., Imoto, K., Sakmann, B., 1996. Ca^2+ buffering and action potential-evoked Ca^{2+} signaling in dendrites of pyramidal neurons. Biophys. J. 70, 1069–1081.

Jafri, M.S., Yang, K.-H., 2003. Modeling neuronal calcium dynamics. In: Feng, J.F. (Ed.), Computational Neuroscience–A Comprehensive Approach. CRC, London.

LeMasson, G., Marder, E., Abbott, L.F., 1993. Activity-dependent regulation of conductances in model neurons. Science 256, 1915–1917.

Pinsky, P.F., Rinzel, J., 1994. Intrinsic and network rhythmogenesis in a reduced Traub model for CA3 neurons. J. Comput. Neurosci. 1, 39–60.

De Schutter, E., Smolen, P., 1998. In: Koch, C., Segev, I. (Eds.), Methods in Neuronal Modeling: From Ions to Networks. The MIT Press, Cambridge, MA, pp. 211–250.

Smith, G.D., Cox, C.L., Sherman, S.M., Rinzel, J., 2001. A firing-rate model of spike-frequency adaptation in sinusoidally-driven thalamocortical relay neurons. Thalamus Related Syst. 11, 1–22.

Wang, X.J., 1998. Calcium coding and adaptive temporal computation in cortical pyramidal neurons. J. Neurophysiol. 79, 1549–1566.